Proceedings of the
Annual Stability Conference
Structural Stability Research Council
Orlando, Florida, April 12-15, 2016

Influence of Plate Stiffener Geometry on LTB Capacity

Piyachai Chansuk[1], Aaron G. Freidenberg[2], Craig E. Quadrato[3], Megan M. Rogers[4]

Abstract
The standard analytical equations for elastic and inelastic lateral-torsional buckling assume a connection that permits rotation about the strong axis (as well as warping), but prevents twist about the longitudinal axis. The plate stiffener, commonly called a shear tab, is idealized as such a connection. In this paper, the influence of plate stiffener geometry on the lateral-torsional buckling capacities of various wide-flange beams is studied, using high-fidelity computer simulation. Preliminary results indicate that plate stiffener geometries have a significant effect on beam LTB capacity.

Keywords: Distortion, twist, shear tab, plate stiffener, lateral torsional buckling

1. Research Significance

The current equations for lateral torsional buckling (LTB) capacity conservatively assume that flexural members' end connections allow warping (Fig. 1) and rotation about the strong axis. Other assumptions idealize the connecting elements (also known as shear tabs) as restricting twist and distortion (Fig. 2) at the ends of flexural members. However, in reality, shear tab performance may not meet these assumptions. The equations also assume that the geometry of shear tabs has no effect on LTB capacity. Mensinger's experimental work shows that beams with a small span over depth (L/d) ratio can be sensitive to shear tab geometry (2014). The significance of the current research is that it further investigates the influence of shear tab geometry on LTB capacity, and identifies favorable shapes of shear tabs.

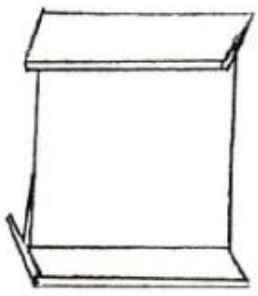

Figure 1: Warping in a Beam (Quadrato)

[1] Student, United States Military Academy, <piyachai.chansuk@usma.edu>
[2] Assistant Professor, United States Military Academy, <aaron.freidenberg@usma.edu>
[3] Academy Professor, United States Military Academy, <craig.quadrato@usma.edu>
[4] Student, United States Military Academy, <megan.rogers@usma.edu>

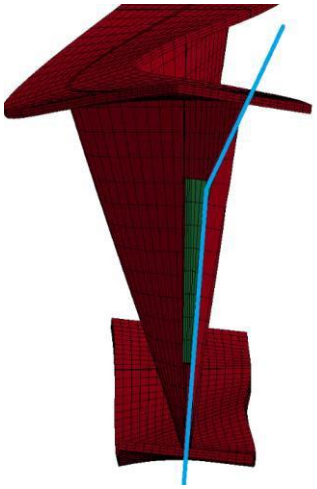

Figure 2: Beam Experiencing Distortion

2. LTB Analytical Equations

In the case of a simply supported doubly symmetric member subjected to a uniform moment, Timoshenko and Gere (1961) developed closed-form equations under the assumptions that the ends of the flexural member are prevented from lateral deflection and twisting, but free to rotate about the strong and weak axes and are free to warp (Ziemian, 2010). Solving the governing differential equations gives the critical bucking moment as (Johnston, 1976)

$$M_{ocr} = \frac{\pi^2 EI_y}{L^2}\frac{h_0}{2}\sqrt{1+\frac{1}{W^2}} \tag{1}$$

where h_0 is the distance between the flange centroids and

$$W = \frac{\pi}{L}\sqrt{\frac{EC_w}{GJ}} \tag{2}$$

where the square-root term in Eq. 2 represents the effect of warping torsional stiffness (Ziemian, 2010).

More refined calculations were developed to account for attachment of lateral or torsional bracing components to the ends of the flexural members (Ziemian, 2010). However, the effect of plate connection geometry itself has never been included in any calculations. Regardless of plate connection geometry, all shear tabs are assumed to provide the ideal displacement boundary conditions as described above. This research compares the performance of long-thin shear tabs against short-thick shear tabs in meeting the ideal connection characteristics.

3. Model

3.1 General

The research utilizes a high-fidelity finite element software, LS-DYNA, to model a wide flange shape girder connected to columns via single-plate connections and simulate a quasi-static

loading condition on the flexural member to obtain its LTB moment capacity. To study the influence of shear tab geometries on LTB capacity, the research team ran many simulations with different wide flange shapes and plate connection geometries in order to build a holistic data base. Each simulated girder was composed of 10,000 8-noded solid elements. Each node can translate in three directions—x, y, and z, thus a total of 24 translation degrees of freedom per element. The constitutive relation of each element is governed by generalized Hooke's Law in three dimensions. A quasi-static displacement control approach was used to load the girder.

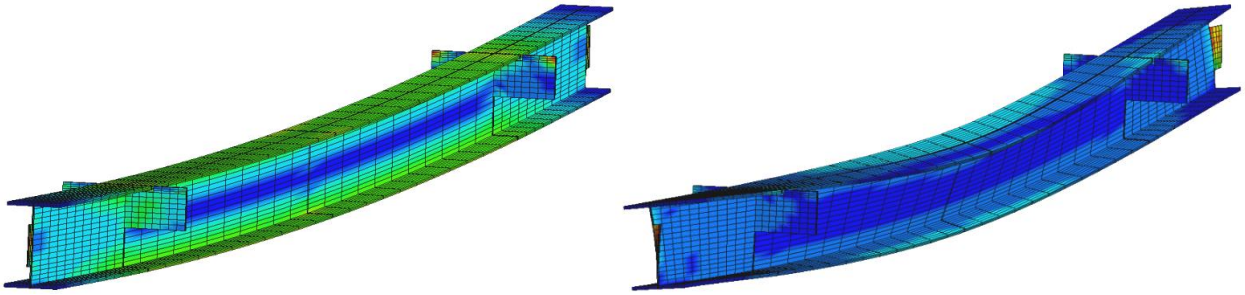

Figure 3: Loaded girder from LS-DYNA (left indicates a girder prior to LTB and right depicts the same girder failed due to LTB)

3.2 Research Design

The research conducted two simulations on each selected W-flange member: the first simulated a girder with long-thin shear tabs as end connections (Fig. 4a), the second simulated a girder with short-thick shear tabs as end connections (Fig. 4b). All shear tab geometries considered are permitted per AISC (2011) and were chosen based on the maximum expected end shear in the girder at the girder's LTB capacity. In each simulation, the girder is subjected to quasi-static loading condition until failure. Under quasi-static loading condition, inertial effects are negligible. Force-time histories of vertical forces that are imparted to the girder from the connecting parts were used for determining a time-history of bending moment. Data was collected to study the influence of shear tab geometry on a member's LTB capacity.

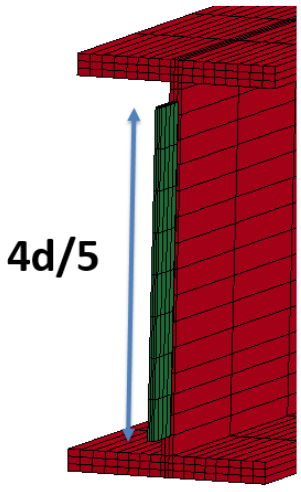

Figure 4a: Long-thin shear tab

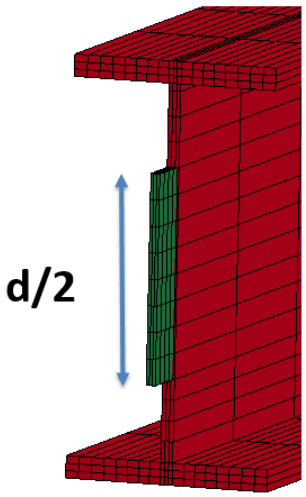

Figure 4b: Short-thick shear tab

3.3 Shear Tab Boundary Conditions and Geometries

This model simulates a girder that is connected to webs of columns on both ends via single plate connections welded to the column web and bolted to the supported girder, constituting flexible support conditions. The nodes of shear tab elements are allowed to translate in the longitudinal direction, but not in lateral or vertical directions. This is different from the nodes of the secondary beams, where the model restrains translation in the longitudinal and lateral direction, and prescribes translation in the vertical direction. All shear tabs in the simulations have an eccentricity of 3.5 inches. The depth of each long-thin shear tab equals 4/5 of girder's depth. Short-thick shear tab's depth equals 1/2 of girder's depth. Shear tabs' thicknesses vary based on required shear strength.

3.4 Loading Configuration

The model depicted a simply-supported girder subjected to two equal concentrated loads symmetrically placed $0.25L_b$ distance away from both ends (Fig. 5). This configuration yields uniform bending moment along the middle section of the girder (lateral-torsional buckling modification factor C_b equal to unity). In the simulation the girder is loaded using displacement control – i.e. prescribed vertical displacements of the secondary members, as described in the previous section on boundary conditions.

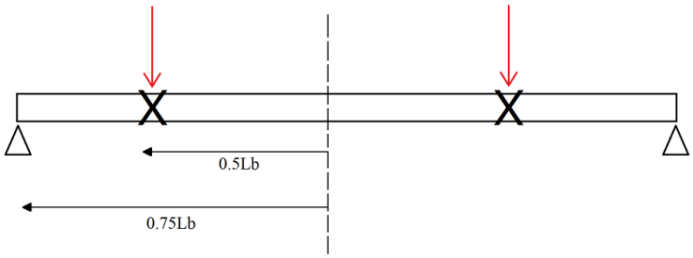

Figure 5: Simulation Configuration

4. Members Selection

9 different depths of wide-flange shape (W14, 16, 18, 21, 24, 27, 30, 33, and 36) were selected to include both short and tall members. This research focused on elastic LTB only, so unbraced lengths were chosen accordingly. In selecting the weight of the members, the team identified the heaviest member for each depth that elastic LTB capacity could be found. Then, the team selected lighter shapes to be analyzed in the simulations. In summary, 44 members were selected as listed in Table 1. Because each selected W-flange member was simulated twice with two different kinds of plate connections (short/thick and long/thin), a total of 88 simulations were studied, each loaded until elastic LTB failure was observed.

Table 1: Selected Members

	W14	W16	W18	W21	W24	W27	W30	W36
Weight (lb/ft)	53	57	50	55	55	84	90	170
	61	67	71	62	68	94	99	
	68	77	86	73	84	102	116	
	82	100	106	83	103	129	132	
			130	93	117	161	173	
				122	146	178	211	
				147	176	217	261	
					207	258		
Total	4	4	5	7	8	8	7	1

5. Results and Discussion

5.1 Categorization of Selected Members

According to Fig 6a, 6b, and 6c, there are two distinct groups of members—members with low depth to flange width ratio ($d/b_f < 2.1$) and members with high depth to flange width ratio ($d/b_f > 2.3$). Each selected wide flange depth has data points represented by both groups except for W14 and W36 (all W14 members had $d/b_f < 2.1$ and only one W36 was studied, which fell under the second group category).

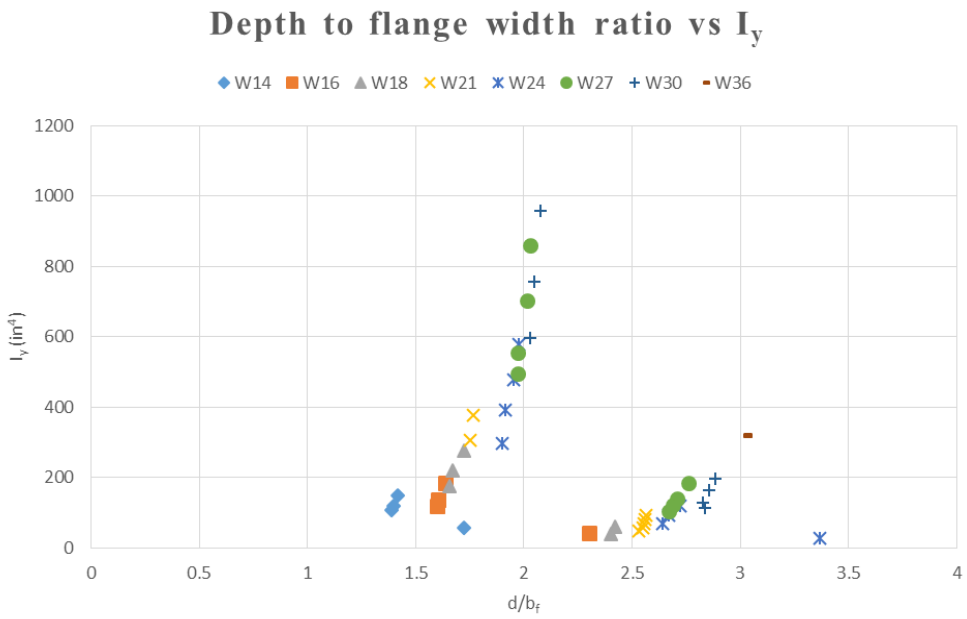

Figure 6a: Depth to flange width ratio v. weak axis moment of inertia plot

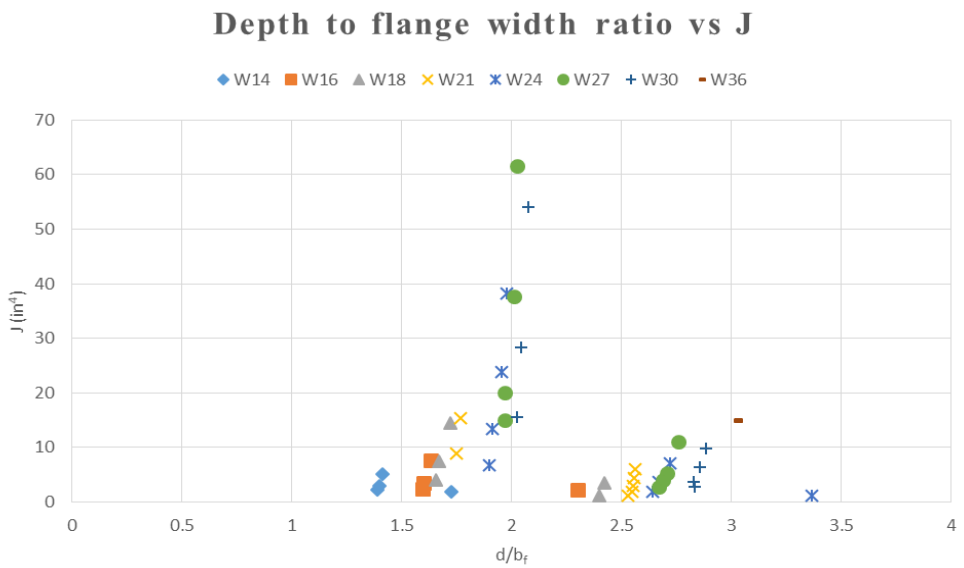

Figure 6b: Depth to flange width ratio v. torsional resistance constant plot

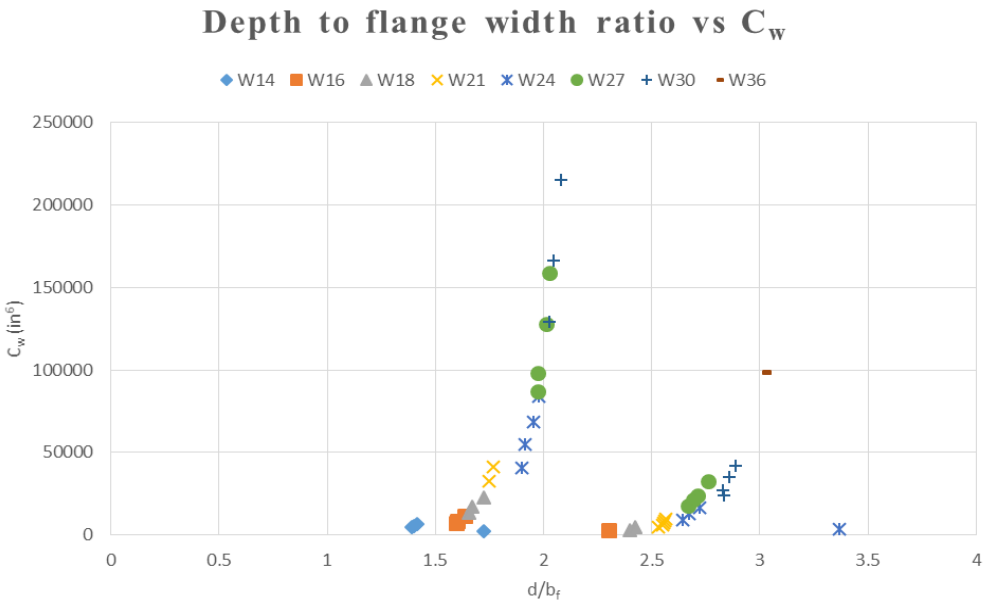

Figure 6c: Depth to flange width ratio v. wrapping resistance constant plot

Looking at each wide flange depth individually, almost every member in the low d/b_f group has higher values of geometric constants (weak-axis moment of inertia I_y, torsional resistance constant J, and warping resistance constant C_w) than the members in the high d/b_f group. This trend is more noticeable in deeper shapes (W21, W24, W27, and W30).

The plots also depict relatively small ranges of geometric constant values in W14, W16, and W18 shapes. For example, considering all J values of W16 members, the range of the data is 5.51 in^4 (13.26 in^4 for W18). On the contrary, W27's range of J values is 58.79 in^4 (51.26 in^4 in W30). Indeed, the data points of W14, W16, and W18 shapes lie relatively close together in comparison to data points of W21, W24, W27, and W30. Therefore, all W14, W16, and W18

members are considered as one general group with relatively similar geometric property regardless of their d/b_f ratios.

Thus, the d/b_f ratio of 2.5 was used to clearly categorize the W21, W24, W27, W30, and W36 data points into two groups—the low and high d/b_f ratio groups. In each of these W-flange shapes, the members in low d/b_f ratio group tend to have higher geometric constant values in relative to the members in the other group.

5.2 Influence of Plate Connections

For each selected member (recall that there were 44 member chosen in total), the two simulations varied only in the geometries of the shear tabs (the first one had long-thin shear tabs as plate connections and the second one simulated short-thick shear tabs). However, each pair of simulations yielded two different LTB moment capacities. For Fig. 7, the long-thin shear tab simulation (M_{thin}) was considered the initial value, while the LTB moment that resulted from the short-thick shear tab simulation (M_{thick}) was considered as the changed value. Percent change was calculated for each member and plotted against d/b_f as shown in Fig. 7.

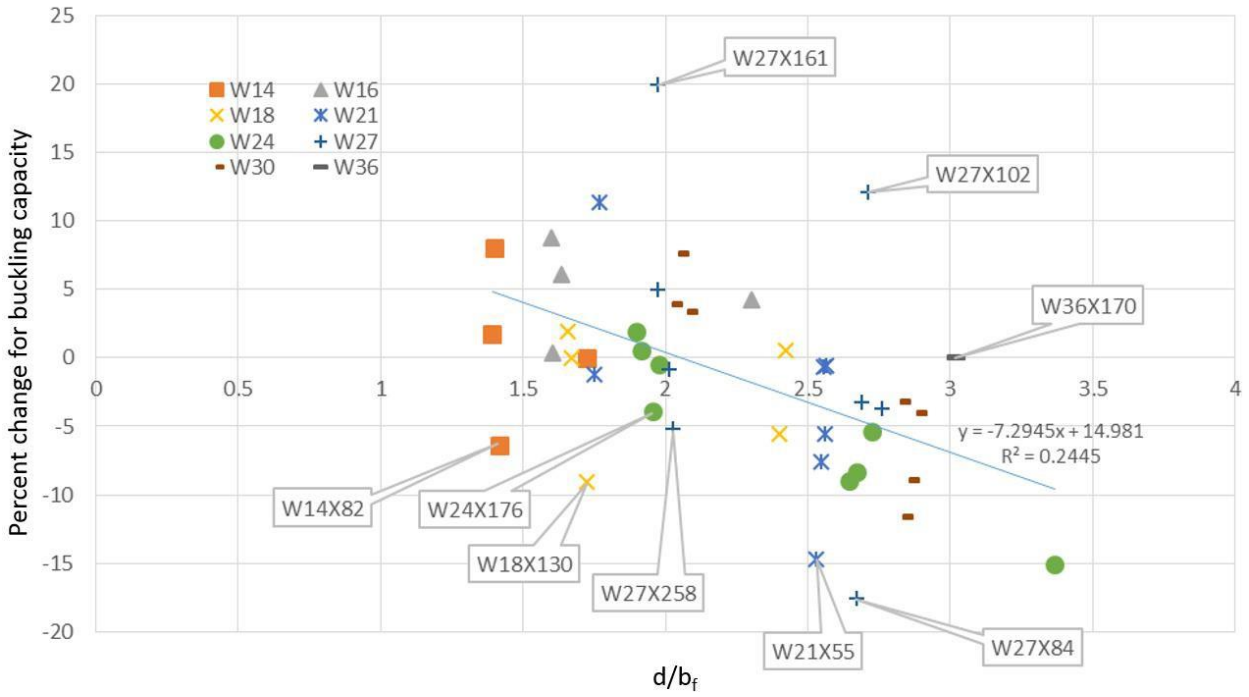

Figure 7: Plot of percent change v. d/b_f

Generally, the data points establish a negative relationship with $R^2 = 0.2445$; percent change decreases and becomes negative as d/b_f ratio increases. Noticeably, almost every member with a high d/b_f ratio ($d/b_f > 2.5$) performs worse when plate connection geometry changes from a long-thin shape to a short-thick shape.[5]

[5] Only W27X102 and W36X170 have positive percent change among all other members whose d/b_f ratios are greater than 2.5

The LTB analytical equations assume ideal connections that do not allow twist or distortion at flexural member's ends. In reality, performances of plate connections hardly meets this idealized assumption. This research objectively compares the performances of long-thin shear tabs against short-thick shear tabs in meeting the ideal connection characteristics.

Looking at the cross-sectional properties of the girder itself, tall-thin cross sections are more prone to distortion relative to short-wide cross sections. Based on this observation, long shear tabs should be more effective in stabilizing movements at connection ends of tall-thin members. Truly, Fig. 6 depicts that long-thin shear tabs are crucial for tall-thin members. When short-thick shear tabs were used in the simulations of tall-thin members, LTB capacities drop—the average percent decrease from initial M_{thin} is -5.93% for members with $d/b_f > 2.5$.[6] In a group of data points whose $d/b_f > 2.5$, there are two outliners—W27X102 and W36X170. W36X170 has a relatively high d/b_f ratio and should have lower LTB moment when switch from long to short shear tabs. However, the data indicates that changing from long to short shear tabs has a minor and opposite effect on W36X170 LTB capacity (0.06% increase). This can be explained by the member's relatively high I_y, J, and C_w values in comparison to other tall-thin members with approximate d/b_f ratios of 2.8. The relatively high numbers of these constants are the indicators of a highly LTB resistive member. It should not be a surprise that shear tab geometry matters less for a member of this type. The W27X102 member, with a d/b_f ratio of 2.71, does not, at present, have an explanation for its inconsistent behavior.

Looking at the data holistically, a clear trend cannot be established among the data points whose $d/b_f < 2.5$. In general, the use of short-thick shear tabs can either increase or decrease an LTB capacity of a member in this category.

As discussed in section 5.1, members of W14, W16, and W18 shapes have relatively low and close geometric constant values regardless of which d/b_f ratio group they reside in. Comparing these data points with other members whose I_y, J, and C_w values are also relatively low (among the high d/b_f ratio group of W21, W24, W27, and W30 shapes), the W14, W16, and W18 members do not behave the same way as others. Indeed, using short-thick shear tabs for connections does not always negatively impact the LTB moment capacity of these members. However, it is important to note that all of their d/b_f ratios are less than 2.5. In other words, we are not yet able to *a priori* predict the influence of connection geometry for short-wide members with low I_y, J, and C_w values. However, as the members' d/b_f ratios increase (the girders become more slender), proper connection geometry can be predicted, as previously explained.

In conclusion, short-thick shear tabs are not suitable for slender (high d/b_f ratio) members whose I_y, J, and C_w values are small. However, though a member has small geometric constant values, short-thick shear tabs do not necessarily have negative impact on LTB capacity if that member is stocky (has low d/b_f ratio).

6. Conclusions

The current use of LTB analytical equations does not account for shear tab geometries in calculating LTB critical moments. The results from the high-fidelity finite element analysis

[6] The average percent decrease becomes -7.42% when exclude the outliners (W27X102 and W36X170) from the calculation

simulations indicate that the shapes of the shear tabs used significantly affect critical bucking moments. In 21 members out of 44 selected members, percent differences between the moments developed in long-thin shear tab simulations and the moments developed in short-thick shear tab simulations are greater than 5% (see Fig. 8).

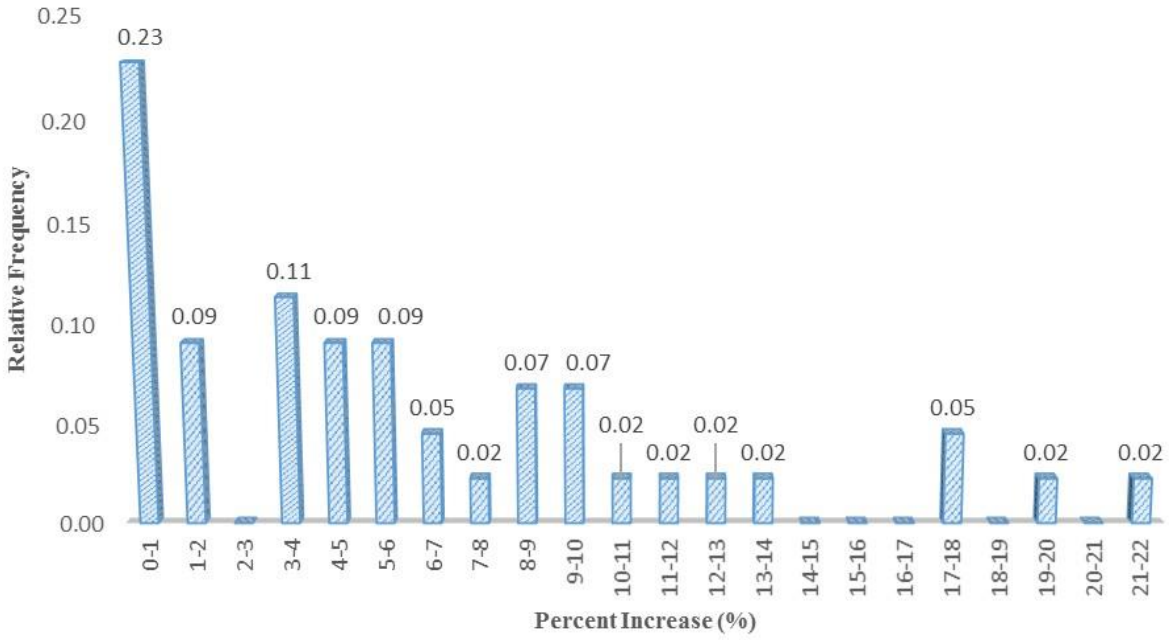

Figure 8: Relative Frequency Distribution of Percent Difference between M_{thin} and M_{thick}

Further analysis indicates that short-thick plate connections can provide a benefit for members with a stocky cross-section, but are not suitable for members with relatively narrow flanges compared to the section depth. In addition to having tall-thin cross sections, these slender members tend to have relatively low cross-sectional constants I_y, J, and C_w, in comparison to members of the same depth section that have flange width to section depth ratios d/b_f closer to 1.0. Indeed, W-flange members that reside in this category (high d/b_f) have higher performance when long-thin shear tabs are used as end connections. Further research is recommended to verify this trend and investigate the causal factors.

In addition, future studies should consider improving the model used in the simulation to limit external factors that do not pertain to the study's objectives. In the current model, adjacent segments may have provided additional end restraint to the most critical unbraced segment in the center, causing a substantial increase in the member's LTB capacity (Nethercot and Trahair, 1976; Nethercot, 1983). Therefore, to limit this continuity effect, the adjacent unbraced segments of this model could be excluded from the new model in order to create an isolated unbraced length, which can be accomplished by simply removing some of the boundary conditions on the secondary beams. Since the current model does not suffer from load height effects as the loads are applied at the members' webs, the loading conditions can remain the same, but the restraints from the secondary beams can be removed.

Acknowledgments
The high-fidelity simulations were performed using U.S. Department of Defense High Performance Computing (HPC) Modernization Program systems.

References
American Institute of Steel Construction (AISC) (2011), Steel Construction Manual (Fourteeth Edition), *United States of America*.

Johnston, B. G. (Ed.) (1976), *Guide to Stability Design Criteria for Metal Structures*, Wiley, New York.

Mensinger, M., & Möller, H. (2014, September). Influence of Hinged Connections on Lateral-Torsional Buckling of Single-Span Beams. In Eurosteel 2014.

Nethercot, D. A. (1983), "Elastic Lateral Buckling of Beams,'' in *Beams and Beam Columns: Stability in Strength* (Ed. R. Narayanan), Applied Science Publishers, Barking, Essex, *England.*

Nethercot, D. A, and Trahair, N. S. (1976), "Lateral Buckling Approximations for Elastic Beams," Struct. Eng., *Vol. 54, No. 6, pp. 197–204.*

Quadrato, C. (2014), "Increasing Girder Elastic Buckling Strength Using Split Pipe Bearing Stiffeners," in *Journal of Bridge Engineering*, American Society of Civil Engineers.

Timoshenko, S. P., and Gere, J. M. (1961), *Theory of Elastic Stability*, McGraw-Hill, New York.

Ziemian, Ronald D., ed. *Guide to Stability Design Criteria for Metal Structures.* Sixth Edition. John Wiley & Sons, Inc., 2010. Print.